iASPP, a microRNA-124 target, is aberrantly expressed in astrocytoma and regulates malignant glioma cell migration and viability

XIANGRONG LIU[1,2], JUN KANG[3], SI SUN[3], YUMIN LUO[1], XUNMING JI[1], XIANWEI ZENG[4] and SHANGFENG ZHAO[3]

[1]Cerebrovascular Diseases Research Institute and [2]China-America Joint Institute of Neuroscience, Xuanwu Hospital of Capital Medical University, Beijing 100053; [3]Department of Neurosurgery, Beijing Tongren Hospital, Capital Medical University, Beijing 100730; [4]Department of Neurosurgery, The Affiliated Hospital of Weifang Medical College, Weifang, Shandong 261031, P.R. China

Received October 3, 2016; Accepted October 6, 2017

DOI: 10.3892/mmr.2017.8097

Abstract. MicroRNAs (miRNAs) regulate biogenesis and disease development by targeting numerous mRNAs. miRNA (miR)-124 and its direct target, inhibitor of apoptosis-stimulating protein of p53 (iASPP), may be involved in tumor development and progression. The aim of the present study was to explore the role of miR-124-targeted iASPP in glioma. The results demonstrated that miR-124 was aberrantly expressed in astrocytic glioma tissue and in the human glioblastoma cell lines U87 and U251. The expression of miR-124 was lower in astrocytic gliomas compared with normal brain (NB) tissues, with a more reduced expression in higher-grade tumors. In addition, several miR-124 loci (including miR-124-1, miR-124-2 and miR-124-3) were revealed to be more highly methylated in U87 cells compared with methylation levels in U251 cells and NB cells. Furthermore, the expression of iASPP was higher in high-grade astrocytic gliomas compared with low-grade astrocytic gliomas. miR-124 overexpression effectively inhibited U87 and U251 cell migration. In addition, miR-124 regulated cell viability and arrested the cell cycle at the G0/G1 phase in these two cell lines. miR-124 also reduced the expression levels of the cell cycle related genes iASPP, cyclin-dependent kinase (CDK)4, CDK6 and cyclin D1. Results from the present study indicated that expression of the miR-124 target gene iASPP may contribute to glioma development and progression.

Correspondence to: Dr Shangfeng Zhao, Department of Neurosurgery, Beijing Tongren Hospital, Capital Medical University, 1 Dong Jiao Min Xiang, Beijing 100730, P.R. China
E-mail: zshangfeng@126.com

Dr Xianwei Zeng, Department of Neurosurgery, The Affiliated Hospital of Weifang Medical College, 2428 Yuhe Road, Weifang, Shandong 261031, P.R. China
E-mail: zengxianwei15@163.com

Key words: glioma, cell cycle, microRNA, methylation, migration, inhibitor of apoptosis-stimulating protein of p53

Introduction

Gliomas are the most common primary brain tumors in adults (1). Astrocytomas are a type of glioma that are graded between I and IV according to a World Health Organization (WHO) grading system, which is determined following pathological evaluation of the tumor. Low-grade gliomas (WHO grade I and II) are well differentiated with a good prognosis, whereas high-grade gliomas (WHO grade III and IV) are malignant with a poor prognosis (2).

MicroRNAs (miRNAs) are small noncoding RNAs that function as negative regulators of posttranscriptional gene expression by binding with the 3'untranslated regions of target mRNAs to either inhibit their translation or promote degradation (3,4). Altered miRNA expression has been associated with cancer development and drug resistance (5). Ectopic miRNA expression may aid in cancer diagnosis, prognosis and therapy, and may predict possible responses to treatment (6). miRNA (miR)-124 is highly conserved in animals and is the most abundantly expressed miRNA in the embryonic and adult brain, serving a key role in neurogenesis (7-9). A recent study reported that miR-124 expression is downregulated in a variety of human cancers, and is therefore considered to be a tumor suppressor (10). miR-124 was also demonstrated to inhibit the migration and invasion of glioma cells, and reduced miR-124 expression may be predictive of a poor prognosis in patients with gliomas (11-13). miR-124 has numerous mRNA targets that are related to the cell cycle, oncogenesis and cancer metastasis (14-16), such as cyclin-dependent kinase (CDK)6, inhibitor of apoptosis-stimulating protein of p53 (iASPP) and IQ motif containing GTPase activating protein 1 (IQGAP1) (17-19). iASPP is involved in cancer metastasis and is a promising therapeutic target (20,21). Although miR-124 targeting of iASPP has been implicated in glioma progression (22), the specific role remains to be elucidated.

In the present study, the expression levels of miR-124 and iASPP were examined in human glioma tissues and in human U251 and U87 glioma cell lines. In addition, the methylation status of miR-124 in U251 and U87 cells was examined and

functional analyses of miR-124 in these cells were conducted. The results suggested that miR-124 may serve as a molecular biomarker for glioma tumors of different grades and may represent a novel therapeutic target for the treatment of gliomas.

Materials and methods

Patients and cell lines. All samples were collected from Beijing Tongren Hospital (Beijing, China) between 2011 and 2014, and were stored in liquid nitrogen until use. Patients with glioma (n=66) and normal control patients (n=14) were examined following receipt of written informed consent, and this study was approved by The Ethics Committees of Beijing Tongren Hospital, Capital Medical University (Beijing, China). Gliomas were diagnosed and graded based on the WHO classification system, and of the 66 glioma tissues collected, 19 were classified as diffuse astrocytoma (grade II), 25 as anaplastic astrocytoma (grade III) and 22 as glioblastoma multiforme (grade IV). The clinicopathological information of all glioma patients is presented in Table I. A total of 14 healthy normal brain (NB) tissues were collected from patients receiving treatment of cerebral injury by internal decompression and treatment of epilepsy by temporal lobe resection (9 male and 5 female, 8 <50 years old, 6 ≥50 years old).

The human glioblastoma cell lines U87 and U251 were purchased from Peking Union Medical College (Beijing, China) and maintained in Dulbecco's modified Eagle's medium supplemented with 10% fetal bovine serum (Sigma-Aldrich; Merck KGaA, Darmstadt, Germany), 10 U/ml penicillin and 0.1 mg/ml streptomycin (Sigma-Aldrich; Merck KGaA), at 37˚C and 5% CO_2.

Reverse transcription-quantitative polymerase chain reaction (RT-qPCR). For RT-qPCR, 0.1 g tissues and $5x10^6$ cells were used to extract total RNA using the mirVana miR Isolation kit (Ambion; Thermo Fisher Scientific, Inc., Waltham, MA, USA), according to the manufacturer's protocols. The mature form of miR-124 was detected using the miRNA RT kit (Applied Biosystems; Thermo Fisher Scientific, Inc.) and TaqMan Universal PCR Master Mix (Applied Biosystems; Thermo Fisher Scientific, Inc.), according to the manufacturer's protocols. The primers were used as previously described (23). Reverse transcription reactions were incubated for 10 min at 16˚C, 30 min at 37˚C and 5 min at 65˚C. The real-time PCR protocol was used as follows: 95˚C for 2 min, followed by 40 cycles at 95˚C for 15 sec, 60˚C for 60 sec and 70˚C for 30 sec. U6 was used as an internal control. qPCR was performed using the CFX Connect Real-Time PCR Detection System (Bio-Rad Laboratories, Inc., Hercules, CA, USA) and analyzed using CFX Maestro Software, Chinese edition (12005260; Bio-Rad Laboratories, Inc.). The relative quantitative value for each target gene was performed using the $2^{-\Delta\Delta Cq}$ method (24).

Oligonucleotide transfection. miR-124 mimics and miRNA-negative control were purchased from Life Technologies (Thermo Fisher Scientific, Inc.). The sequence of the miR-124 mimics was 5'-UAAGGCACGCGGUGA AUGCC-3' and the miR-negative control sequence was 5'-UUGUACUACACAAAAGUACUG-3'. U251 and U87 cells ($3.5x10^5$ cells/well) were seeded into 6-well plates and transfected when the cells reached 60% confluence; 50 nmol/l miR-124 mimics and miRNA-negative control were transfected as previously described (25) using Lipofectamine RNAiMAX (Thermo Fisher Scientific, Inc.), following the manufacturer's protocol. The medium was removed and fresh growth medium was added 6 h after transfection at 37˚C; cells were incubated for 36 h at 37˚C prior to collection for analysis. Three independent repeats were performed for all experiments.

Bisulfite sequencing PCR. U87 and U251 cells ($6x10^5$) and NB astrocytes were treated with the MethylCode Bisulfite Conversion kit (Thermo Fisher Scientific, Inc.) according to the manufacturer's protocols. Genomic DNA was extracted using the QIAamp DNA Mini kit (Qiagen, Hilden, Germany) according to the manufacturer's protocols. PCR was performed using TaqMan Universal PCR Master Mix (Thermo Scientific, Inc.). The primer sequences are listed in Table II. PCR amplification was conducted with the following parameters: initial denaturation at 95˚C for 3 min, followed by 40 cycles of 95˚C for 30 sec, 60˚C for 30 sec and 72˚C for 40 sec, followed by 1 cycle of 72˚C for 5 min. The amplified fragments were cloned into the pMD18-T vector (Takara Bio, Inc., Tokyo, Japan) and 8 clones were randomly selected for sequencing (Invitrogen; Thermo Scientific, Inc.).

Immunofluorescence staining. Tissues were fixed using 4% Paraformaldehyde for 24 h at room temperature. Immunofluorescence staining was performed on formalin-fixed/paraffin-embedded sections (4 μm), as previously described (18). Primary antibodies include rabbit anti-iASPP polyclonal antibody (ab34898; 1:100; Abcam, Cambridge UK), mouse anti-glial fibrillary acidic protein (GFAP) monoclonal antibody (MAB360; 1:100; EMD Millipore, Billerica, MA, USA) or mouse anti-neuronal nuclei (NeuN) monoclonal antibody (MAB377; 1:100; EMD Millipore). Cy3 donkey anti rabbit IgG (711-165-152; 1:800; Jackson Immunoresearch, West Grove, PA, USA) and Alexa Fluor 488 donkey anti mouse IgG (715-545-150; 1:800; Jackson Immunoresearch) were used as secondary antibodies. Cell nuclei were stained with DAPI (Invitrogen; Thermo Fisher Scientific, Inc.). Sections were observed under a fluorescence microscope (Carl Zeiss AG, Oberkochen, Germany). Four fields were detected per slide.

Cell viability assay. The effects of miR-124 on cell proliferation were determined by MTT assay. MTT (Sigma-Aldrich; Merck KGaA) was dissolved in distilled H_2O (5 mg/ml) and sterilized through a 0.22-μm filter. Briefly, U87 and U251 cells ($3x10^3$ cells/well) were seeded into 96-well plates and transfected at 24 h after seeding. At 0, 24, 48, 72 and 96 h following transfection, cells were incubated at 37˚C and 20 μl MTT solution was added to each well and cells were incubated for 2 h at 37˚C. Following removal of the medium, the colored formazan product was then dissolved in 150 μl dimethylsulfoxide. Optical density was measured at 570 nm using a microplate reader (Bio-Rad Laboratories, Inc.). Triplicate wells were assayed for each time point.

Cell cycle analysis. At 48 h following miRNA transfection at 37˚C, $1x10^6$ U87 and U251 cells were collected and fixed

Table I. Clinicopathological features of 66 glioma patients.

Clinicopathological feature	WHO II	WHO III	WHO IV
Cases (n)	19	25	22
Sex			
Male	11	15	14
Female	8	10	8
Age			
<50	10	13	10
≥50	9	12	12
KPS score			
<80	4	11	9
≥80	15	14	13
Tumor size			
<5 cm	12	15	17
≥5 cm	7	10	5

KPS, Karnofsky performance status; WHO, World Health Organization.

Table II. Primer sequences used for bisulfite genomic sequencing.

Primer	Sequence (5'→3')	Size (bp)
P1	F: GGGGATTTAGTYGTATTATATA	297
	R: TAAAAACRAAACCCATCTAA	
P2	F: ATTATTTGGGATTTGAGYGA	255
	R: CTACTTCRCCCAAAAAACTAAA	
P3	F: TTAGTTTTTTGGGYGAAGTAGA	264
	R: CCAAAAACTCTTTATTCTCCCC	
P4	F: TTTGTAGGAAAAAGTTTGGAT	300
	R: AAAAAAAAACCTTTCTCCTAAA	
P5	F: GGGTTTTTGYGTAAGATTAGTT	258
	R: ACTCCTCAACCAATAACCACA	
P6	F: TAGATTGTGGTTATTGGTTGAG	228
	R: TCATCTTTCTTTATAATACRAAAAAA	
P7	F: GGGAAGTTTTAGTGAGTAGGTTT	306
	R: AACCATTACCAATCATTTTCTACTA	
P8	F: TTTTTAAGGATATTTYGGGGAG	270
	R: ACCCCRAAAAAAAAACCA	
P9	F: GTTTGGTTTTTTTTTYGG	315
	R: TACTCAAAAATAAAAACTCRTCTC	
P10	F: GAGAYGAGTTTTTATTTTTGAGT	276
	R: AAAAAATAAACCCCCAAAT	
P11	F: TTGGGGGTTTATTTTTTGT	257
	R: ACATTAAATCAAAATCCRCTAT	

P, primer; R, A or G nucleotide; Y, C or T nucleotide.

overnight in 70% ethanol at 4˚C and subsequently treated with 0.5 mg/ml RNase in PBS at 37˚C for 30 min. Cell nuclei were stained with 50 μg/ml propidium iodide at 4˚C for 30 min. Cells ($1x10^6$) were analyzed for their DNA content using BD FACSDiva software version 8.0.1 (BD Biosciences, Franklin Lakes, NJ, USA) in a BD Influx flow cytometer (BD Biosciences).

Western blot analysis. Western blotting was performed as previously described (26). Briefly, ~0.5 g of tissue was used to extract the protein. The protein concentration was determined by a Bicinchoninic Acid Protein Assay kit (Pierce; Thermo Fisher Scientific, Inc.), using bovine serum albumin (Pierce; Thermo Fisher Scientific, Inc.) as the standard. Protein samples (100 μg/lane) were separated by 8 or 10% SDS-PAGE and subsequently transferred to polyvinylidene fluoride membranes (EMD Millipore). Following blocking in 5% skimmed milk for 2 h at room temperature, the membranes were incubated overnight at 4˚C with the following antibodies: rabbit anti-CDK4 polyclonal antibody (sc-260; 1:200; Santa Cruz Biotechnology, Inc., Dallas, TX, USA), mouse anti-CDK6 polyclonal antibody (3136; 1:1,000; Cell Signaling Technology, Inc., Danvers, MA, USA), rabbit anti-iASPP polyclonal antibody (ab34898; 1:1,000; Abcam), rabbit anti-Cyclin D1 polyclonal antibody (sc-717; 1:200; Santa Cruz Biotechnology, Inc.) and rabbit anti-β-actin polyclonal antibody (sc-7210; 1:5,000; Santa Cruz Biotechnology, Inc.). β-actin was used as an internal loading control. Membranes were subsequently incubated with horseradish peroxidase-conjugated goat anti-rabbit secondary immunoglobulin G-horseradish peroxidase (HRP) (sc-2004; 1:2,000; Santa Cruz Biotechnology, Inc.) or goat anti-mouse secondary immunoglobulin G-HRP (sc-2005; 1:2,000; Santa Cruz Biotechnology, Inc.) in blocking solution for 1 h at room temperature. Protein bands were visualized by Western Chemiluminescent HRP Substrate (EMD Millipore). Protein expression levels were normalized to the β-actin loading control. The relative optical density of protein bands was measured following subtraction of the film background using Image-Pro Plus version 6.0 (Media Cybernetics, Inc., Rockville, MD, USA).

Wound-healing assay. Cells were seeded into 6-well plates at a density of $8x10^5$ cells per well. At 24 h after seeding, miR-124 mimics and miR-negative controls were transfected into cells with at least 70% confluence in 6-well plates. Following 6 h transfection, cell layers were scratched using a 200 μl sterile pipette tip to form wound gaps and washed immediately with serum-free medium twice. Wounds were measured at 0 and 24 h. Images of the wound width were captured for 6 fields in each well and analyzed using Image-Pro Plus 6.0 (Media Cybernetics, Inc.). Relative migration rate=(start distance-end distance)/start distance.

Statistical analysis. Group distributions were compared parametrically using the Student's t-test or by one-way analysis of the variance with Scheffe's post hoc test; group distributions were compared non-parametrically using the Mann-Whitney U-test. All analyses were done using GraphPad Prism software version 5.01 (GraphPad Software, Inc., La Jolla, CA, USA). $P<0.05$ was considered to indicate a statistically significant difference.

Results

Expression of miR-124 in astrocytic glioma tissues and cell lines. The expression levels of miR-124 were quantified by RT-qPCR in 66 astrocytoma (grade II, 19; grade III, 25; grade IV, 22), 14 healthy NB control tissues and the glioma cell lines, U87 and U251 (Fig. 1). miR-124 expression was significantly lower in the three astrocytic glioma tissues compared with NB controls (P<0.001). The expression level of miR-124 in low-grade gliomas (grade II) was significantly higher compared with expression in the high-grade gliomas (P<0.05 vs. grade III; P<0.01 vs. grade IV), whereas miR-124 expression was lower in grade IV gliomas compared with grade III (P<0.05). miR-124 expression in gliomas is not influenced by gender or age (data not shown). These results indicated that the downregulation of miR-124 may be related to the degree of malignancy of the glioma, and suggested a putative crucial role for downregulation of miR-124 in the initiation and progression of glioma. Although U87 and U251 are both human glioblastoma cell lines and demonstrated low expression level of miR-124, the expression level of miR-124 in U87 cells was significantly lower compared with U251 cells (Fig. 1; P<0.01).

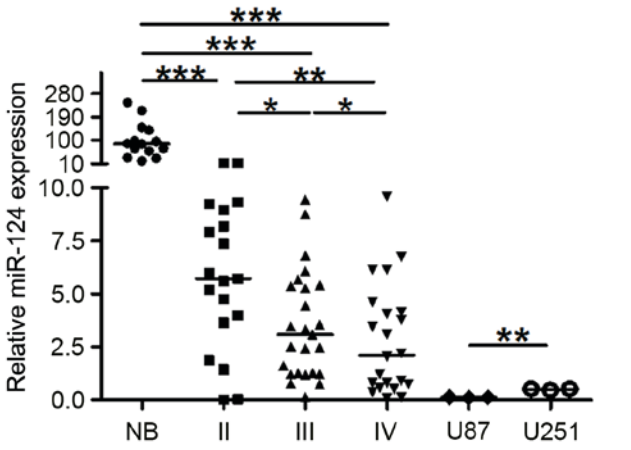

Figure 1. Expression of miR-124 in differently graded astrocytic gliomas and glioma cell lines. miR-124 expression was measured by reverse transcription-quantitative polymerase chain reaction in astrocytic glioma grade II (n=19), grade III (n=25), grade IV (n=22), healthy NB control tissues (n=14) and two glioma cell lines, U87 and U251. -, median value; *P<0.05; **P<0.01; ***P<0.001. miR, microRNA; NB, normal brain.

Methylation of the miR-124 promoter in U87 and U251 cells. The present study also investigated whether the difference in the expression level of miR-124 between U87 and U251 cells was due to methylation status of the miR-124 promoter. It has been predicted that more than 90% of the human miRNA promoters are located 1,000 bp upstream of DNA sequence which can be transcribed to the mature miRNA. (27). miR-124 is transcribed from three loci: hsa-miR-124-1, has-miR-124-2 and has-miR-124-3. Thus, PCR primers were designed in the 1,000 bp upstream region flanking the miR-124 sequence. These sequences flanking hsa-miR-124-1, has-miR-124-2 and has-miR-124-3 were located in gi|224589820:c9761982-9760983, gi|224589820:65290706-65291705 and gi|224589812:61808852-61809851, respectively (https://www.ncbi.nlm.nih.gov/gene; Fig. 2A). Bisulfite genomic sequencing results confirmed the hypomethylation of miR-124-1, miR-124-2 and miR-124-3 CpG islands in astrocytes from human control tissues and hypermethylation of miR-124-1, miR-124-2 and miR-124-3 in U87 and U251 cells (Fig. 2B). miR-124 loci were more highly methylated in U87 cells compared with U251 cells. These methylation data were consistent with the RT-qPCR result in these cells, which demonstrated low expression of miR-124 in U87 cells and relatively high expression in U251 cells.

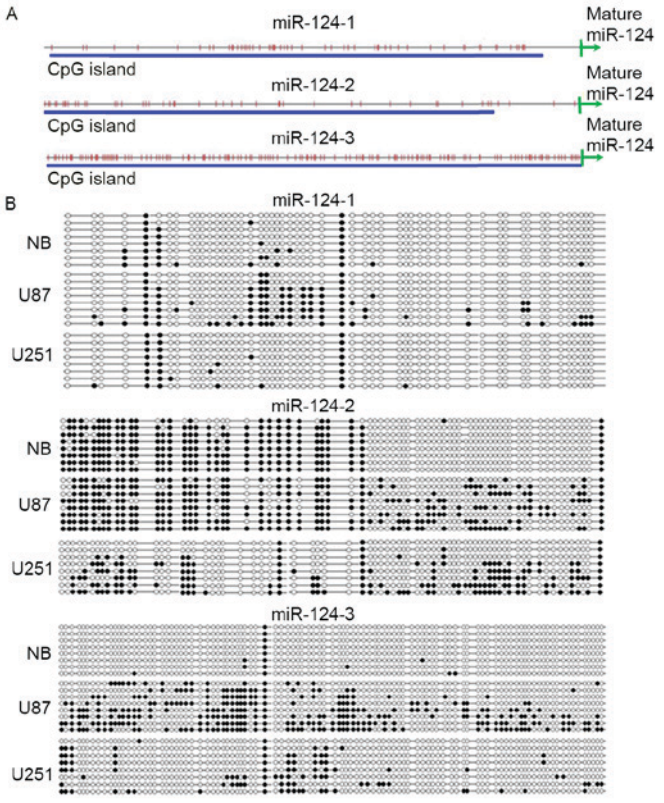

Figure 2. Methylation status of miR-124 loci. (A) Schematic diagram indicating the distribution of CpG dinucleotides (vertical tick marks) flanking the DNA sequence which transcribes to mature miR-124. Blue boxes represent the CpG islands. (B) Bisulfite genomic sequencing of the bisulfite-treated promoter region of miR-124-1, miR-124-2 and miR-124-3 in healthy NB tissue, and U87 and U251 cells. Empty circles indicate unmethylated and filled circles indicate methylated CpG dinucleotides in the eight independent clones per sample. miR, microRNA; NB, normal brain.

Expression of iASPP protein in astrocytic glioma tissues. To determine the relationship between the expression of iASPP and astrocytoma grades, iASPP protein expression levels were detected by western blotting and immunofluorescence. The result demonstrated that iASPP protein expression levels significantly increased with advancing WHO gliomas grade (Fig. 3A). However, the protein expression level of iASPP was significantly lower in WHO grade I glioma compared with NB control (P<0.05). The cellular distribution of iASPP was examined by immunofluorescence staining. iASPP expression was almost undetected in astrocytes from NB, while gradually increased in Grad II to Grade IV astrocytomas. Highly positive staining of iASPP was observed in the neurons of NB (Fig. 3B and C).

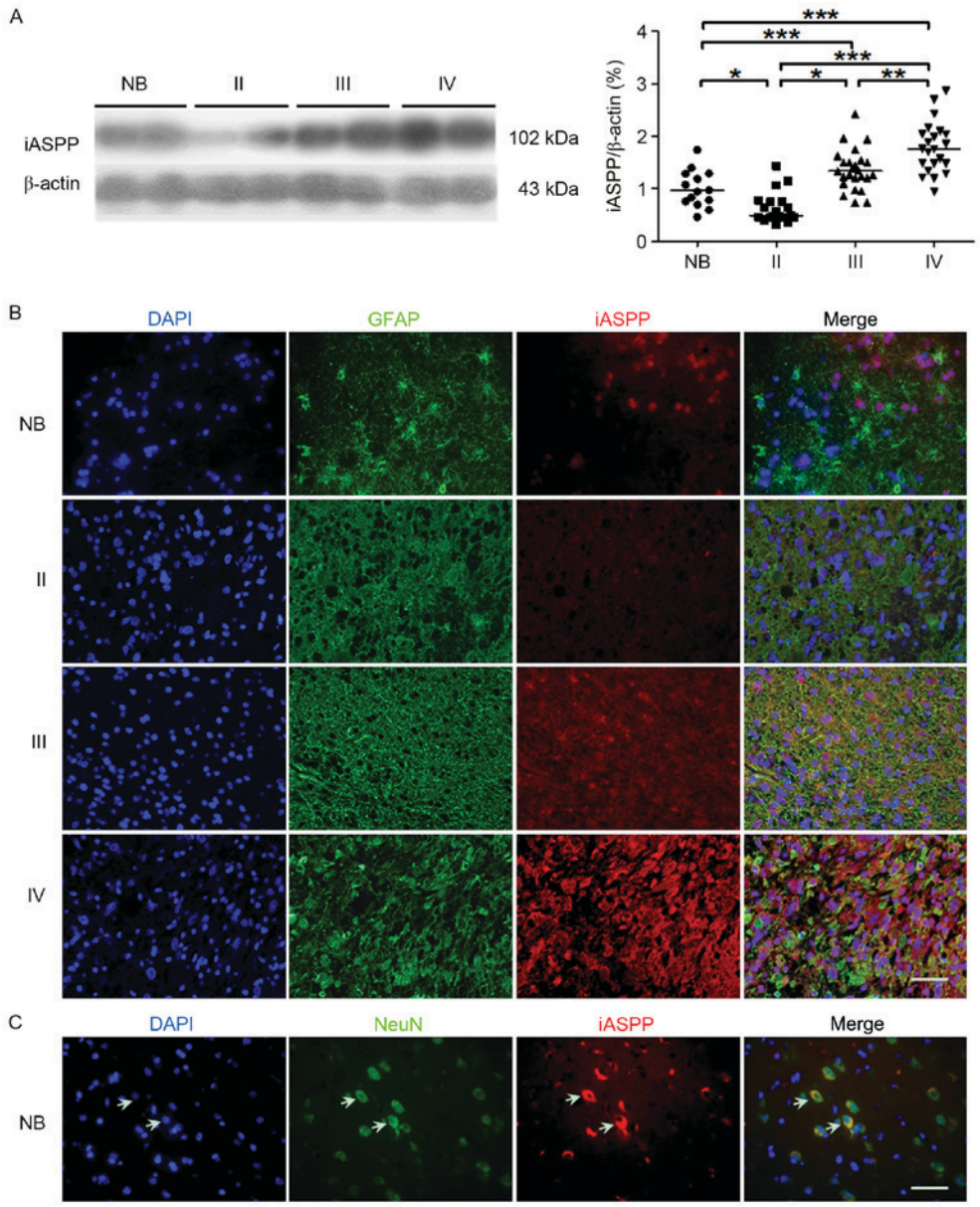

Figure 3. Expression of iASPP protein in different grade gliomas. (A) Representative western blotting image of iASPP expression in patients with different grade astrocytic glioma and healthy NB controls, and subsequent densitometric analysis; β-actin was used as a loading control. Median values are indicated; *P<0.05; **P<0.01; ***P<0.001. (B) Representative immunofluorescence staining for iASPP (red) and GFAP (green) in patients with different grade astrocytic glioma. GFAP is a marker for astrocytes; nuclei were stained with DAPI. (C) Representative immunofluorescence staining for iASPP (red) and NeuN (green) in NB controls. NeuN is a marker for neurons; nuclei were stained with DAPI. Arrows indicate representative neurons. Scale, 50 μm. GFAP, glial fibrillary acidic protein; iASPP, inhibitor of apoptosis-stimulating protein of p53; NB, normal brain; NeuN, neuronal nuclei.

miR-124 inhibits U87 and U251 cell migration. To confirm the effects of miR-124 on the glioma cell migration, wound-healing assays were performed in U87 and U251 cells that were transfected with miR-124 mimics or miR-negative control oligonucleotides. The results revealed that miR-124 mimics significantly inhibited wound closure in U87 and U251 cells compared with cells in the miR-negative control groups (P<0.05; Fig. 4). These results indicated that the upregulation of miR-124 expression attenuated the migratory ability of glioma cells.

miR-124 inhibits cell viability and induces cell-cycle arrest in glioma cells. To determine whether miR-124 affects cell growth and proliferation, MTT assays and cell cycle distribution assays were performed. Compared with the miR-negative control group, U87 cells transfected with miR-124 mimics exhibited reduced viability at 48 and 72 h post-transfection (P<0.05; Fig. 5A). miR-124 mimics transfection significantly inhibited cell viability in U251 cells at 48 h compared with cells transfected with the miR-negative control oligonucleotides (P<0.05; Fig. 5B).

The cell cycle status was analyzed in U87 and U251 cells using the flow cytometer 48 h post-transfection with miR-124 mimics or miR-negative control (Fig. 5C-F). The percentage of cells at S phase cells was significantly lower in miR-241 mimics transfected U87 cells (21.0±5.7%) compared with the percentage of S phase cells in the miR-negative control group (33.8±4.1%; P<0.05; Fig. 5C and D), whereas the

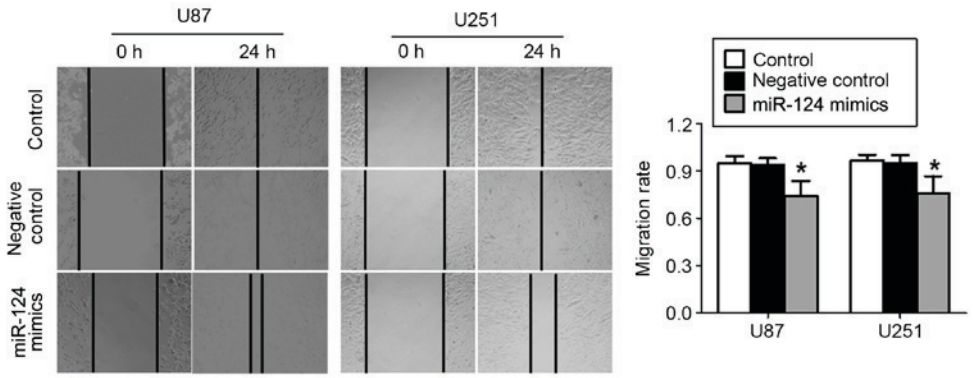

Figure 4. Effects of miR-124 on U87 and U251 cell migration. Representative images of the wound-healing assays at 0 and 24 h post-transfection with miR-124 mimics or miR-negative control oligonucleotides, and the calculated migration rates. The wound gaps were analyzed by measuring the distance of migrating cells for six regions of each wound. Data are presented as the mean ± standard deviation; n=3; *P<0.05. The control group is untransfected cells. miR, microRNA.

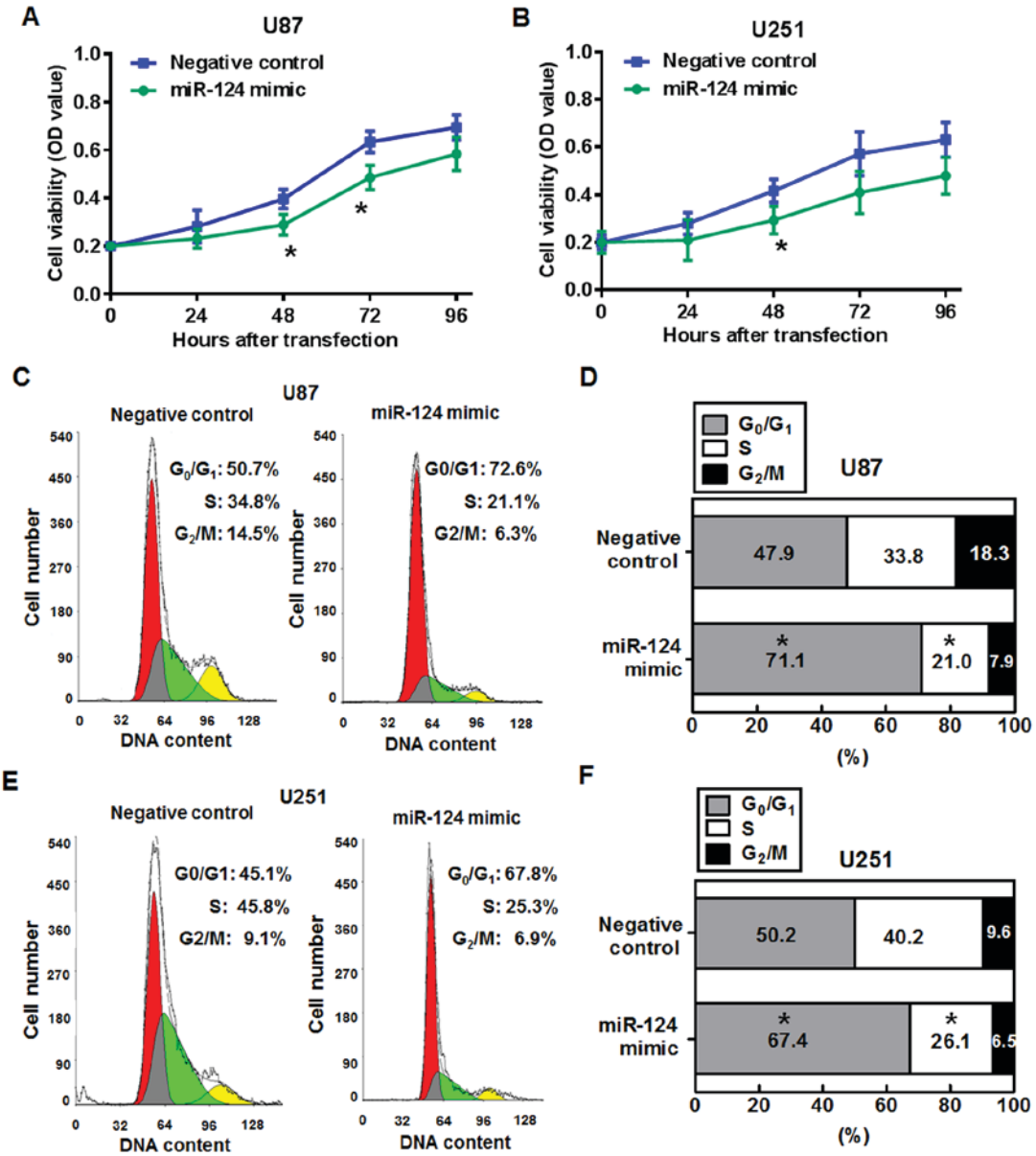

Figure 5. Effects of miR-124 mimic on the viability of U87 and U251 cells. The viability of (A) U87 and (B) U251 cells transfected with miR-124 mimics or miR-negative control oligonucleotides; Data are presented as the mean ± standard deviation; n=9. (C) Representative cell cycle distributions and (D) average proportion of the cells in each phase in U87 cells transfected with miR-124 mimics or miR-negative control. (E) Representative cell cycle distributions and (F) average proportion of the cells in each phase in U251 cells transfected with miR-124 mimics or miR-negative control. n=4/group; *P<0.05. miR, microRNA.

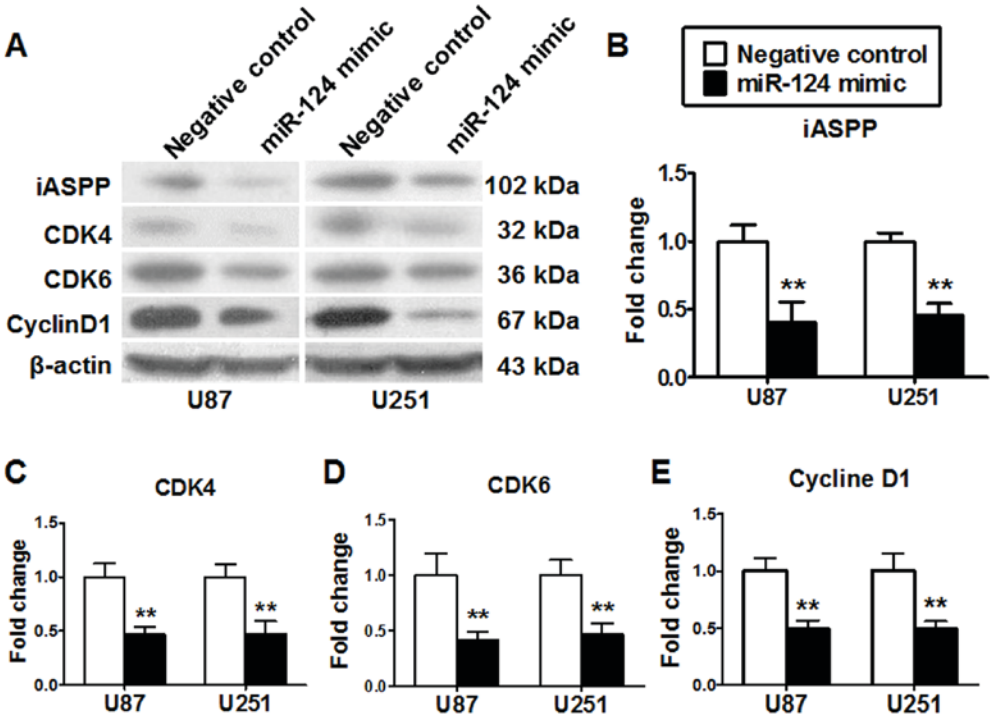

Figure 6. (A) Transfection of miR-124 mimics leads to downregulation of iASPP, CDK4, CDK6 and Cyclin D1 protein expression levels. Quantification of (B) iASPP, (C) CDK4, (D) CDK6 and (E) Cyclin D1 expression in U87 and U251 cells was conducted by densitometric analysis. β-actin served as an internal control. Data are presented as the mean ± standard deviation; n=4; **P<0.01. CDK, cyclin-dependent kinase; iASPP, inhibitor of apoptosis-stimulating protein of p53; miR, microRNA.

percentage of G0/G1 phase cells was significantly higher in miR-124 mimics transfected cells (71.1±6.9%) compared with the miR-negative controls (47.9±3.8%; P<0.05). Similarly, the proportion of U251 cells in the S-phase fraction was significantly lower following miR-124 mimics transfection (26.1±5.7%) compared with miR-negative control transfection (40.2±5.9%; P<0.05; Fig. 5E and F), and the proportion of cells in the G_0/G_1 phase was significantly higher in themiR-124 mimics treated group (50.2±3.8%) compare with the miR-negative control group (67.4±6.9%; P<0.05). These results suggested that the reduction in cell viability at 48 h may occur through cell cycle arrest.

miR-124 inhibits the expression of target gene associated with cell cycle regulation. The effects of miR-124 on the expression of its target genes were determined by western blot. The protein expression levels of the miR-124 target genes CDK4, CDK6 and iASPP, and cell cycle regulatory protein cyclin D1 were examined in U87 and U251 cells 48 h post-transfection with miR-124 mimics or miR-negative control. The results demonstrated that miR-124 mimics transfection led to decreased expression levels of CDK4, CDK6, iASPP and cyclin D1 in U87 and U251 cells compared with cells transfected with the miR-negative control oligonucleotides (P<0.01; Fig. 6).

Discussion

miR-124 is a tumor suppressor, and its expression is significantly decreased in many types of cancer (28,29). miR-124 expression has been reported to decrease tumor initiation, promotion and progression in different cell culture systems and in animal models (11-13). In the present study, reduced expression of miR-124 was observed in astrocytoma tissue, with a more pronounced reduction in high-grade gliomas, which was consistent with previous reports (11,12). These findings indicated that the low expression levels of miR-124 may be involved in the pathological progression of astrocytoma.

Epigenetic silencing of miRNAs together with their target tumor suppressors is becoming a common hallmark of human tumors (30). DNA methylation-based silencing is functionally involved in carcinogenesis (31). Epigenetic silencing of miR-124 by hypermethylation of CpG islands frequently occurs in different tumors, including leukemia, lung cancer and colon cancer (28). The present study demonstrated that the expression level of miR-124 was lower in U87 cells compared with U251 cells, which may be due to a higher level of methylation in the miR-124 promoter region in U87 cells. A recent study demonstrated that miR-124 expression is upregulated in glioblastoma cell lines following treatment with a combination of 5-aza-2'-deoxycytidine (decitabine), a DNA demethylating agent, and trichostatin A (TSA), a histone deacetylase inhibitor, whereas no significant difference in expression was observed in cells treated with decitabine or TSA alone (31). These data suggested that the expression of miR-124 was not regulated by DNA methylation alone, but by a variety of epigenetic modifications. Further investigations are required to define the full extent of DNA methylation that affects miR-124 expression in glioma cell lines and tumors.

As a direct target of miR-124, iASPP is involved in cellular processes, including cell cycle, apoptosis and

autophagy (32-34). iASPP is upregulated in a number of tumors, such as leukemia, lung cancer and hepatocellular carcinoma (35-37). In the present study, iASPP was expressed at low levels in the astrocytes of NB tissue, whereas expression was high in NB neurons, which may be the reason that the expression level of iASPP is higher in NB tissues compared with astrocytoma Grade II. The present study did not detect the expression of iASPP in astrocytes of NB tissue by western blotting; therefore, thorough investigations need to be conducted to explore the expression and role of iASPP both in astrocytoma cells and in all kinds of cell types of NB.

Results from the present study demonstrated that miR-124 may be involved in regulating cell viability and migration in human glioblastoma cells. Overexpression of miR-124 resulted in significant changes in cell migration and viability, and miR-124 may regulate glioblastoma cell viability by arresting the cell cycle at the G0/G1 phase. The cell cycle is tightly regulated by a number of molecular pathways and checkpoints, which may be altered in tumors. miR-124 has a variety of mRNA targets that are associated with the cell cycle, such as CDK6, iASPP and CDK4 (17,18,38). In this study, the results of these previously published reports were confirmed; further suggesting that miR-124 may influence the cell cycle in glioma cells. CDK4, CDK6 and iASPP have recently been identified as direct targets of miR-124 (17,18,38). iASPP was reported to downregulate the expression of cyclin D1 (32), which controls the transition from the G1 phase to the S phase. Another direct target of miR-124 is IQGAP1 (not examined by the present study), which is suppressed by miR-124 leading to a downregulation of β-catenin and downstream cyclin D1 expression (19).

In conclusion, the present results indicated that miR-124 is downregulated in glioma cells and this reduced expression level may promote tumor growth and progression. In addition, miR-124 may serve as a potential biomarker for pathological diagnosis and represents a promising therapeutic target for the treatment of glioma.

Acknowledgements

The authors thank Yanglong Li and Kaiyuan Song (Beijing Tongren Hospital, Capital Medical University, Beijing, China) for collecting tissue samples. This work was supported by The National Natural Science Foundation of China (grant nos. 81000504, 81471209 and 81641055) and The Beijing Natural Science Foundation (grant no. 7132112).

References

1. Goodenberger ML and Jenkins RB: Genetics of adult glioma. Cancer Genet 205: 613-621, 2012.
2. Dunbar E and Yachnis AT: Glioma diagnosis: Immunohistochemistry and beyond. Adv Anat Pathol 17: 187-201, 2010.
3. Shenoy A and Blelloch RH: Regulation of microRNA function in somatic stem cell proliferation and differentiation. Nat Rev Mol Cell Biol 15: 565-576, 2014.
4. Lin S and Gregory RI: MicroRNA biogenesis pathways in cancer. Nat Rev Cancer 15: 321-333, 2015.
5. Garofalo M and Croce CM: Role of microRNAs in maintaining cancer stem cells. Adv Drug Deliv Rev 81: 53-61, 2015.
6. Jiang C, Chen X, Alattar M, Wei J and Liu H: MicroRNAs in tumorigenesis, metastasis, diagnosis and prognosis of gastric cancer. Cancer Gene Ther 22: 291-301, 2015.
7. Lagos-Quintana M, Rauhut R, Yalcin A, Meyer J, Lendeckel W and Tuschl T: Identification of tissue-specific microRNAs from mouse. Curr Biol 12: 735-739, 2002.
8. Kloosterman WP, Wienholds E, de Bruijn E, Kauppinen S and Plasterk RH: In situ detection of miRNAs in animal embryos using LNA-modified oligonucleotide probes. Nat Methods 3: 27-29, 2006.
9. Cao X, Pfaff SL and Gage FH: A functional study of miR-124 in the developing neural tube. Genes Dev 21: 531-536, 2007.
10. Cao Q, Li YY, He WF, Zhang ZZ, Zhou Q, Liu X, Shen Y and Huang TT: Interplay between microRNAs and the STAT3 signaling pathway in human cancers. Physiol Genomics 45: 1206-1214, 2013.
11. Chen T, Wang XY, Li C and Xu SJ: Downregulation of microRNA-124 predicts poor prognosis in glioma patients. Neurol Sci 36: 131-135, 2015.
12. Shi Z, Chen Q, Li C, Wang L, Qian X, Jiang C, Liu X, Wang X, Li H, Kang C, *et al*: MiR-124 governs glioma growth and angiogenesis and enhances chemosensitivity by targeting R-Ras and N-Ras. Neuro Oncol 16: 1341-1353, 2014.
13. An L, Liu Y, Wu A and Guan Y: microRNA-124 inhibits migration and invasion by down-regulating ROCK1 in glioma. PLoS One 8: e69478, 2013.
14. Shkumatava A, Stark A, Sive H and Bartel DP: Coherent but overlapping expression of microRNAs and their targets during vertebrate development. Genes Dev 23: 466-481, 2009.
15. Clark AM, Goldstein LD, Tevlin M, Tavaré S, Shaham S and Miska EA: The microRNA miR-124 controls gene expression in the sensory nervous system of Caenorhabditis elegans. Nucleic Acids Res 38: 3780-3793, 2010.
16. Chi SW, Zang JB, Mele A and Darnell RB: Argonaute HITS-CLIP decodes microRNA-mRNA interaction maps. Nature 460: 479-486, 2009.
17. Pierson J, Hostager B, Fan R and Vibhakar R: Regulation of cyclin dependent kinase 6 by microRNA 124 in medulloblastoma. J Neurooncol 90: 1-7, 2008.
18. Liu X, Li F, Zhao S, Luo Y, Kang J, Zhao H, Yan F, Li S and Ji X: MicroRNA-124-mediated regulation of inhibitory member of apoptosis-stimulating protein of p53 family in experimental stroke. Stroke 44: 1973-1980, 2013.
19. Lu SH, Jiang XJ, Xiao GL, Liu DY and Yuan XR: miR-124a restoration inhibits glioma cell proliferation and invasion by suppressing IQGAP1 and β-catenin. Oncol Rep 32: 2104-2110, 2014.
20. Liu Z, Zhang X, Huang D, Liu Y, Zhang X, Liu L, Li G, Dai Y, Tan H, Xiao J and Tian Y: Elevated expression of iASPP in head and neck squamous cell carcinoma and its clinical significance. Med Oncol 29: 3381-3388, 2012.
21. Wang LL, Xu Z, Peng Y, Li LC and Wu XL: Downregulation of inhibitor of apoptosis-stimulating protein of p53 inhibits proliferation and promotes apoptosis of gastric cancer cells. Mol Med Rep 12: 1653-1658, 2015.
22. Zhao WH, Wu SQ and Zhang YD: Downregulation of miR-124 promotes the growth and invasiveness of glioblastoma cells involving upregulation of PPP1R13L. Int J Mol Med 32: 101-107, 2013.
23. Zhang Y, Zheng L, Huang J, Gao F, Lin X, He L, Li D, Li Z, Ding Y and Chen L: MiR-124 Radiosensitizes human colorectal cancer cells by targeting PRRX1. PLoS One 9: e93917, 2014.
24. Schmittgen TD and Livak KJ: Analyzing real-time PCR data by the comparative C(T) method. Nat Protoc 3: 1101-1108, 2008.
25. Wang D, Zhang H, Li M, Frid MG, Flockton AR, McKeon BA, Yeager ME, Fini MA, Morrell NW, Pullamsetti SS, *et al*: MicroRNA-124 controls the proliferative, migratory and inflammatory phenotype of pulmonary vascular fibroblasts. Circ Res 114: 67-78, 2014
26. Liu X, Wang L, Zhao S, Ji X, Luo Y and Ling F: β-catenin overexpression in malignant glioma and its role in proliferation and apoptosis in glioblastoma cells. Med Oncol 28: 608-614, 2011.
27. Zhou X, Ruan J, Wang G and Zhang W: Characterization and identification of microRNA core promoters in four model species. PLoS Comput Biol 3: e37, 2007.
28. Sato F, Tsuchiya S, Meltzer SJ and Shimizu K: MicroRNAs and epigenetics. FEBS J 278: 1598-1609, 2011.
29. Papagiannakopoulos T and Kosik KS: MicroRNAs: Regulators of oncogenesis and stemness. BMC Med 6: 15, 2008.

30. Toiyama Y, Okugawa Y and Goel A: DNA methylation and microRNA biomarkers for noninvasive detection of gastric and colorectal cancer. Biochem Biophys Res Commun 455: 43-57, 2014.
31. Silber J, Lim DA, Petritsch C, Persson AI, Maunakea AK, Yu M, Vandenberg SR, Ginzinger DG, James CD, Costello JF, *et al*: miR-124 and miR-137 inhibit proliferation of glioblastoma multiforme cells and induce differentiation of brain tumor stem cells. BMC Med 6: 14, 2008.
32. Li G, Wang R, Gao J, Deng K, Wei J and Wei Y: RNA interference-mediated silencing of iASPP induces cell proliferation inhibition and G0/G1 cell cycle arrest in U251 human glioblastoma cells. Mol Cell Biochem 350: 193-200, 2011.
33. Cai Y, Qiu S, Gao X, Gu SZ and Liu ZJ: iASPP inhibits p53-independent apoptosis by inhibiting transcriptional activity of p63/p73 on promoters of proapoptotic genes. Apoptosis 17: 777-783, 2012.
34. Chikh A, Sanzà P, Raimondi C, Akinduro O, Warnes G, Chiorino G, Byrne C, Harwood CA and Bergamaschi D: iASPP is a novel autophagy inhibitor in keratinocytes. J Cell Sci 127: 3079-3093, 2014.
35. Deng Q, Sheng L, Su D, Zhang L, Liu P, Lu K and Ma S: Genetic polymorphisms in ATM, ERCC1, APE1 and iASPP genes and lung cancer risk in a population of southeast China. Med Oncol 28: 667-672, 2011.
36. Zhang X, Wang M, Zhou C, Chen S and Wang J: The expression of iASPP in acute leukemias. Leuk Res 29: 179-183, 2005.
37. Lin BL, Xie DY, Xie SB, Xie JQ, Zhang XH, Zhang YF and Gao ZL: Down-regulation of iASPP in human hepatocellular carcinoma cells inhibits cell proliferation and tumor growth. Neoplasma 58: 205-210, 2011.
38. Deng X, Ma L, Wu M, Zhang G, Jin C, Guo Y and Liu R: miR-124 radiosensitizes human glioma cells by targeting CDK4. J Neurooncol 114: 263-274, 2013.